Cross sections for positron and electron collisions with an analog of the purine nucleobases: Indole

Luca Chiari,[1] Antonio Zecca,[2] Francisco Blanco,[3] Gustavo García,[4] and M. J. Brunger[5,6]

[1]*Department of Physics, Tokyo University of Science, 1-3 Kagurazaka, Shinjuku, Tokyo 162-8601, Japan*

[2]*Department of Physics, University of Trento, Via Sommarive 14, 38123 Povo, Trento, Italy*

[3]*Departamento de Física Atómica, Molecular y Nuclear, Universidad Complutense de Madrid, E-28040 Madrid, Spain*

[4]*Instituto de Física Fundamental, Consejo Superior de Investigationes Científicas, Serrano 113-bis, E-28006 Madrid, Spain*

[5]*School of Chemical and Physical Sciences, Flinders University, GPO Box 2100, Adelaide, South Australia 5001, Australia*

[6]*Institute of Mathematical Sciences, University of Malaya, 50603 Kuala Lumpur, Malaysia*

(Received 11 December 2014; published 26 January 2015)

Quantitative information about positron and electron collisions with nucleobases is required in charged-particle track simulations to accurately model and assess any radiation damage at the subcellular level in biological systems. However, scattering experiments have so far been restricted to the pyrimidine nucleobases. In this paper we report on total-cross-section measurements for positron impact on indole, a parent molecule of the purine nucleobases, at impact energies between 1 and 25 eV. We also present theoretical cross sections for elastic and total scattering, positronium formation, electronic excitations, and direct ionization between 1 and 500 eV, as calculated with the independent-atom model with the screening-corrected additivity rule. Rotational excitation cross sections are additionally calculated within a Born framework over that same energy range. A significant discrepancy is found between the measured and computed total cross sections, which cannot be entirely accounted for by the lack of forward-angle-scattering discrimination in the experiment. The present results are also compared to the available theoretical cross sections for the purine nucleobases. In addition, total cross sections for electron-indole collisions computed within our theoretical formalism are provided.

DOI: 10.1103/PhysRevA.91.012711 PACS number(s): 34.80.Bm, 34.80.Gs, 34.80.Uv

I. INTRODUCTION

The assessment of subcellular damage in biomolecular systems has become a subject of topical study over the past decade and a half or so [1]. This is the result of the present widespread use of ionizing radiation in medical practice, for both imaging and therapy, throughout the world [2]. About a decade ago it was estimated that some 2.5×10^9 people were exposed to ionizing radiation each year for diagnoses of disease or abnormal pathology [3], while 5.5×10^6 patients underwent therapeutic irradiations [4]. There can be little doubt that the figures from 2002 would have grown significantly during the intervening years. The primary ionizing radiation in most traditional medical devices consists of either charged (electrons, positrons, protons, or heavy ions) or uncharged (photons or neutrons) particles, which lose their kinetic energy through inelastic interactions with the molecules in human tissue. In doing so they produce a substantial number of secondary charged particles, which in turn also thermalize through energy deposition within the biological medium. Unfortunately, it has been shown that those collisions, even at very low energies of a few eV or sub-eV, may result in genotoxic mutations or oncogene activations [5].

In order to optimize the diagnostic efficacy and to minimize the negative side effects on the patient of medical exposures to ionizing radiation, a high level of accuracy in the theoretical and experimental knowledge of the means through which the radiation interacts with matter is required [4]. This can be achieved through a combined effort of low-energy charged-particle track simulations [6,7] and cross-section and energy-loss measurements looking into charged-particle collisions with a variety of biologically relevant molecules. These include water, the amino acids, and the building blocks of the nucleic acids such as the nucleobases and the phosphate and sugar residues in the backbone and their analogs.

With respect to leptonic collisions with the nucleobases, we note that a fair number of experimental (see, for instance, [8–14]) and theoretical (see, e.g., [14–21]) studies have reported on electron-impact cross sections and low-energy electron-induced DNA damage [22–24]. However, the situation with respect to positron scattering is somewhat poorer, with only a limited number of measurements [20,25–27] and calculations [27–30] being available. In particular, we note that both the experimental and theoretical effort was largely dedicated to the investigation of the pyrimidine bases, such as pyrimidine itself [20,26,30] and uracil [25,27]. Indeed, there is only one computation for positron impact with the purine bases [29], namely, adenine and guanine, and no measurements to validate that calculation. The scarcity of data on those molecules can easily be understood in terms of the theoretical difficulties (large computational resources are needed for the scattering description including the quantum chemical basis set) and experimental challenges (solid substances at room temperature that could decompose at higher temperatures) that those targets pose to their study.

In order to, at least in part, fill in this gap in our present knowledge of positron scattering from the purine bases, here we report on low-energy total-cross-section (TCS) measurements of indole (C_8H_7N), a heterocyclic aromatic organic compound that can be considered as a precursor of those bases (see Fig. 1). As specifically shown in Fig. 1, indole has a bicyclic structure similar to that of the purine nucleobases, namely a benzene ring merged with a pyrrole ring. Although the indole structure is ubiquitous in biology, it plays a key role as the chromophore of tryptophan, an aromatic amino acid that has been subject to numerous previous radiolytic, photophysical, and spectroscopic studies [31,32] owing to its important application as a fluorescence probe in protein studies [33]. In this paper we also present theoretical TCSs, the integral

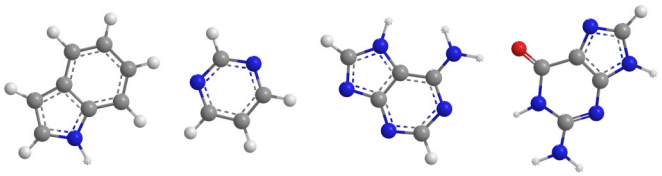

FIG. 1. (Color online) Schematic three-dimensional structures of some important biomolecules. From left to right: indole, pyrimidine, and the purine nucleobases adenine and guanine. Hydrogen atoms are drawn as white, carbon is black, nitrogen is blue, and oxygen is red.

cross sections (ICSs) for elastic scattering, positronium (Ps) formation, electronic excitations and direct ionization, and rotational excitations, as well as elastic differential cross sections (DCSs) for positron-indole collisions. All those cross sections, except for rotational excitations, which use a Born framework, are calculated using the independent-atom model (IAM) with the screening-corrected additivity rule (SCAR) at incident energies between 1 and 500 eV. In addition, we provide the corresponding electron-impact TCS computed using the same theoretical approach.

Investigations into positron interactions with indole are lacking and the existing electron-impact data are very scarce. In this latter respect we mention the electron energy loss and fluorescence spectra of Borisevich *et al.* [34], the ultrafast electron diffraction study of Park *et al.* [32], and the work by Modelli *et al.* [35] on the electron transmission and dissociative electron attachment spectroscopies of indole.

The present paper is organized in the following way. Section II describes the present experimental methods and data analysis procedures, while Sec. III reports the details of our theoretical framework and calculations. The presentation and discussion of our results follow in Sec. IV and the conclusions of the present study are then summarized in Sec. V.

II. EXPERIMENTAL METHODS

The positron spectrometer at the University of Trento was employed to carry out the TCS measurements on indole. That spectrometer, our experimental techniques, and the data analysis procedures have already been described in detail several times (see, e.g., [36]). Hence we only briefly summarize here the information that specifically pertains to the indole measurements. A radioactive ^{22}Na isotope (activity $\sim$1.4 mCi), in conjunction with a tungsten moderator of thickness 1 μm [37], is used to produce a low-energy positron beam. The beam is then transported and focused into the scattering cell by means of some electrostatic optics and a weak axial magnetic field ($B \approx 11$ G). Finally, a channel electron multiplier is used to detect the positrons.

Scattering cross sections are obtained by measuring the transmitted intensity of the positron beam and the pressure in the scattering cell (both with and without the indole vapor), the temperature of the target molecules within the scattering chamber, and the length of the interaction region. By using the Beer-Lambert law [see, e.g., Eq. (1) in Ref. [36]] it is then possible to determine the TCS of interest at each incident energy. We note that some corrections are applied to the data in order to account for some inevitable instrumental effects. In particular, as the operating temperature (45 °C) of the capacitance manometer (MKS 627B) used in the pressure measurements differs from that of the scattering chamber (room temperature), the pressure values are corrected for the thermal transpiration effect [38]. That correction amounts to 4% of the TCS magnitude at most. In addition, the length of the interaction region (scattering cell length of 22.1 $\pm$ 0.1 mm) is corrected for the positrons' effective path increase owing to their gyration in the magnetic field. That latter correction increases the length of the interaction region by 5.5%. Moreover, the transmittance of the positron beam is always kept above 0.7 in order to minimize multiple-scattering events. High-purity (>99%) indole purchased from Sigma-Aldrich was used as the target sample. We also note that preliminary validation measurements on reference targets, such as the noble gases [39–42] or molecular nitrogen [36], were carried out before this experiment in order to check our experimental techniques and procedures.

A retarding potential analysis of the incident beam, without the indole vapor in the chamber, allows for the determination of the energy zero of the positron beam and the beam energy distribution [43]. In doing so we find that the energy resolution of the beam is $\sim$0.25 eV (full width at half maximum) and estimate an uncertainty of $\pm$0.05 eV on the energy scale. Hence, the measured TCSs are actually convoluted over the beam energy distribution, although this effect is expected to be significant only at impact energies below 0.5 eV or so.

The present TCSs are uncorrected for the forward-angle-scattering effect [44], which is expected to be important for a polar molecule such as indole (see Table I). This means that they represent a lower limit on the "true" TCS values. We recall here that the extent of the forward-scattering correction at each given energy depends on the angular discrimination of the apparatus and the shape of the DCSs, for the relevant target species, in this forward angular region. The missing angle of the Trento apparatus is estimated to increase as the incident energy is decreased [36], while the elastic DCSs averaged over the rotational excitations for positron-indole scattering are available from our IAM SCAR calculations (see Fig. 2). In using those DCSs to correct our measured TCSs at a few selected energies, we find that the forward-scattering correction varies from 45% at 1 eV to 13% at 20 eV (see Fig. 3). However, as no independent experimental or theoretical DCSs for indole exists against which we can compare our DCS computations, we have, in general, not applied such a correction.

We note here that the positron beam was somewhat less stable during the indole experiments compared to all our previous measurements on other targets. With other targets the beam was so stable that the beam intensity only changed by a few percent over times of the order of months. However, with indole high stability was achieved only over times of just a few hours. Due to such difficulties, reliable data below 1 eV were not obtained here while for higher energies system stability could not be guaranteed long enough to enable their measurement after acquiring the results between 1 and 25 eV. Indole is solid at room temperature with a vapor pressure of just $\sim$1 Pa [53]. Hence, the target sample was heated to $\sim$45 °C in order to produce a stable source of indole vapor and a sufficient

TABLE I. Some important physicochemical properties of indole, the purine nucleobases adenine and guanine, and pyrimidine.

Property	Indole	Adenine	Guanine	Pyrimidine
permanent dipole moment (D)	2.1 ± 0.1[a]	2.49[d]	2.76[d]	2.33 ± 0.01[f]
dipole polarizability (a.u.)	102[b]	101.2[d]	109.2[d]	58.5[g]
first ionization energy (eV)	7.76[c]	8.26[e]	7.77[e]	9.47[h]
Ps formation threshold energy (eV)	0.96	1.46	0.97	2.67

[a]Reference [45].
[b]Reference [46].
[c]Reference [47].
[d]Reference [48].
[e]Reference [49].
[f]Reference [50].
[g]Reference [51].
[h]Reference [52].

pressure in the scattering chamber. We believe that the reason for the observed positron beam instability might be the fact that indole is a solid electrical insulator at room temperature. Since the entire charged-particle optics and the scattering chamber were at room temperature, indole deposition on the optical active electrodes might inevitably produce electrostatic charging, which in turn causes random deflections of the beam. This may be detected as a beam instability that grows over time as the insulating layer becomes thicker. The positron beam instability is reflected in the statistically larger scatter in the present TCS data and in their larger statistical uncertainties (see below), as well as in the reduced energy span of the present measurements, compared to our earlier measurements on other targets.

The energy range of the present TCS measurements is from 1 to 25 eV. The statistical uncertainties are smaller than 18% and, on average, amount to ∼13%. Other sources of error include the uncertainties in the pressure and temperature measurements (<1% each), in the approach used for the thermal transpiration correction (<2%), and in the length of the scattering region and its correction for the effective positron path length (<3%). The overall errors on the TCSs are therefore estimated to lie within the ∼8%–20% range.

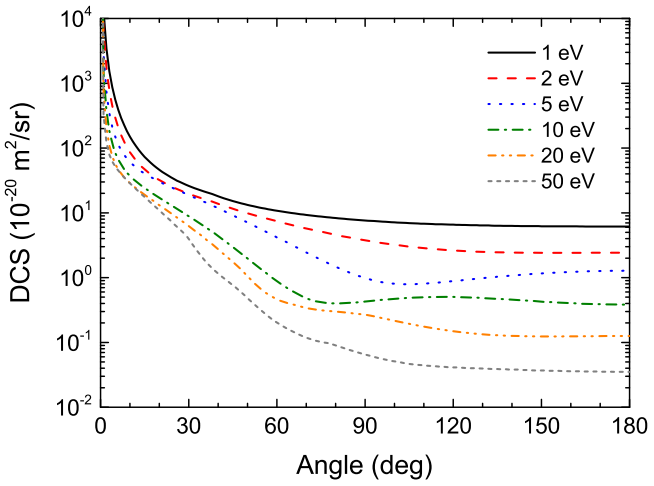

FIG. 2. (Color online) Elastic differential cross sections averaged over the rotational excitations for positron collisions with indole, as calculated with our IAM SCAR and Born approximation methods at incident energies between 1 and 50 eV.

III. THEORETICAL CALCULATIONS

The IAM SCAR method developed by Blanco and Garcia [54] has been recently employed to calculate the cross sections for electron (see, for instance, [55–57]) and positron (see, e.g., [27,30,58,59]) scattering from a variety of large polyatomic molecules and over an extensive energy range, typically from 1 to 1000 eV. Hence, we only briefly reiterate the salient features of that approach here. Our formalism is based on an atomic optical potential model for the individual atoms of the indole molecule, that is, hydrogen, carbon, and nitrogen. For positron collisions the local complex potential is

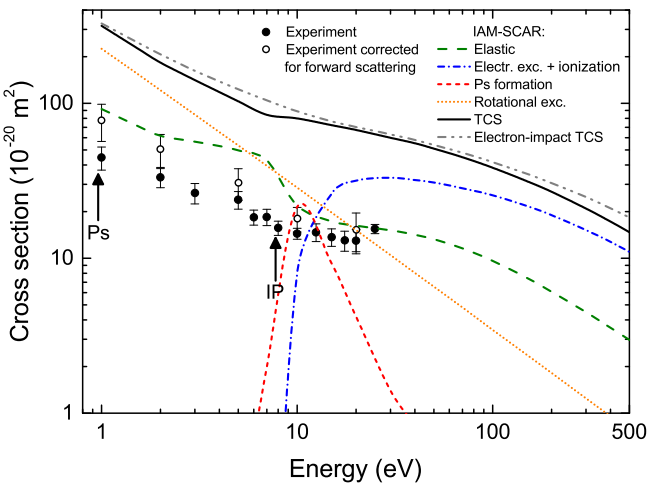

FIG. 3. (Color online) Present experimental total cross sections for positron scattering from indole, both uncorrected and corrected (at a few selected energies) for the forward-angle-scattering effect (see the text). Also plotted are the results of our IAM SCAR calculations of the TCS, ICSs for elastic scattering, ICSs for the electronic excitations plus direct ionization, ICSs for Ps formation, and the Born ICSs for rotational excitations. The calculated electron-impact IAM SCAR TCS is also shown. The black arrows labeled Ps and IP denote the threshold energies for Ps formation and first ionization in indole.

given by

$$V(r) = V_s(r) + V_p(r) + i\,V_a(r). \quad (1)$$

The real part of Eq. (1) drives the elastic-scattering process and includes the electrostatic $V_s(r)$ and polarization $V_p(r)$ interactions. The imaginary part $V_a(r)$ describes all the inelastic processes that are considered as absorptions of flux from the incident positron beam. The static potential was obtained from the charge density derived from Hartree-Fock atomic wave functions, using a similar procedure to that of Reid and Wadehra [60–62]. The dipole plus quadrupole polarization potential was developed from that reported by McEachran *et al.* [63], while the absorption potential accounts for the electronic excitations, Ps formation, and direct ionization. Representing the Ps formation channel is a challenging task and here we have adopted the phenomenological approach introduced in Chiari *et al.* [64].

For electron scattering the complex potential is given by

$$V(r) = V_s(r) + V_{\rm ex}(r) + V_p(r) + i\,V_a(r). \quad (2)$$

In Eq. (2) $V_s(r)$ is the usual Hartree potential of the target, $V_{\rm ex}(r)$ represents the exchange interaction of Riley and Truhlar [65], $V_p(r)$ is the dipole polarization potential of Zhang *et al.* [66], and $V_a(r)$ is the imaginary absorption potential of Staszewska *et al.* [67].

To calculate the cross sections for positron and electron impact with the indole molecule, the additivity rule is then applied to the optical model results for each constituent atom. In this approach, the molecular scattering amplitude stems from the sum of all the relevant atomic amplitudes, including the phase coefficients, which gives the DCSs for the molecule of interest. Integral cross sections can then be determined by integrating those DCSs, with the sum of the elastic and absorption ICSs (for all inelastic processes except rotations and vibrations) then giving the TCS. The geometry of the molecule (atomic positions and bond lengths) is taken into account by using some screening coefficients, which we believe possibly extends the validity of this method down to impact energies of ~30 eV (or lower) for electron and positron scattering.

The IAM SCAR approach described above does not account for vibrational and rotational excitations. However, for polar molecules such as indole (see Table I), additional dipole-induced excitation cross sections can be calculated in the framework of the first Born approximation. These results can then be incorporated into our IAM SCAR calculation in an incoherent way, just by adding up the cross sections as independent channels. The complete approach has already been described in detail [58] and proved to be quite successful when applied to some polar molecules [30,68].

IV. RESULTS AND DISCUSSION

The present experimental TCSs for positron scattering from indole are listed in Table II and shown in Fig. 3. Note that the error bars are just the statistical component (1σ) of the overall uncertainties. We observe in Fig. 3 that the TCS monotonically decreases in magnitude from the lowest investigated energy up to 20 eV. Given the largely polar nature of indole, which has both a very large permanent dipole moment and static dipole polarizability (Table I), the observed TCS behavior is likely to be related to those important intrinsic physicochemical properties of the target. In fact, we have seen in our earlier studies on polar polyatomic species (see, e.g., [58,68–70]) that those properties can play an important role in the low-energy scattering dynamics. This point was also examined in depth by Brunger and Zecca [71]. We also note that indole possesses a very low Ps formation threshold energy (Table I), namely just 0.96 eV. This means that all the present measured TCSs include contributions from that scattering channel. A slight change in the slope of the TCS is manifest at around the first ionization energy (Table I), which might therefore be ascribed to the opening of the direct ionization channel. We also present in Fig. 3 our measured TCSs, corrected for the forward-angle-scattering effect at selected incident energies. We see that this correction only slightly alters the shape of the TCS, most prominently at the lowest energies.

TABLE II. Present experimental total cross sections for positron scattering from indole. The errors represent the statistical uncertainties (1σ).

Energy (eV)	TCS (10^{-20} m^2)	TCS error (10^{-20} m^2)
1.00	44.61	7.58
2.00	33.21	4.67
3.00	26.41	3.98
5.00	23.85	3.12
6.00	18.41	2.03
7.00	18.48	2.23
8.00	15.70	1.65
10.00	14.44	1.17
12.50	14.74	1.93
15.00	13.70	1.77
17.50	13.03	1.93
20.00	13.02	2.34
25.00	15.47	1.06

The results of our IAM SCAR calculations for positron and electron collisions with indole are also plotted in Fig. 3 and are given in numerical form at selected impact energies in Table III. Similar to our experimental TCSs, the calculated positron-impact TCS monotonically decreases in magnitude as a function of increasing the incident energy. At very low energies (<10 eV) the TCS is mostly due to elastic scattering and the rotational excitations, whereas at higher energies direct ionization appears to dominate the scattering process. We observe that the onset of the theoretical Ps formation channel occurs at somewhat higher energies than the known experimental threshold (Table I). As we noted in our earlier studies [55,72], this might reflect an intrinsic limitation in the current theoretical approach for representing the Ps formation channel.

The computed electron-impact TCS shows a very similar behavior to the positron TCS, although it is slightly larger in magnitude at all incident energies. We anticipated this result at the low energies, given the opposite nature of the electrostatic potential in the scattering by the two leptons and the role played by the exchange interaction in electron collisions. We also expected that the positron and electron TCSs would merge at energies of a few hundred eV, i.e., after the Ps formation and electron exchange channels "turn off." Nevertheless,

TABLE III. Present theoretical positron-indole TCS and ICSs for elastic and inelastic (electronic excitations plus direct ionization) scattering, Ps formation, and the rotational excitations calculated with our IAM SCAR and Born approximation methods. Also given is the corresponding theoretical electron-impact TCS.

Energy (eV)	Elastic (10^{-20} m^2)	Inelastic (10^{-20} m^2)	Ps formation (10^{-20} m^2)	Rotational excitation (10^{-20} m^2)	TCS (10^{-20} m^2)	Electron TCS (10^{-20} m^2)
1	91.85	0	0	225.14	316.43	327.63
1.5	72.25	0	0	157.10	229.34	249.79
2	61.61	0	0	121.53	183.14	207.22
3	56.57	0	0	84.57	141.13	161.86
4	52.93	0	0	65.25	118.17	138.33
5	49.57	0	0.16	53.49	103.05	123.21
7	42.84	0	1.98	39.48	84.29	104.45
10	21.90	7.95	21.45	28.56	79.81	88.77
15	17.31	26.01	9.27	19.71	72.25	76.45
20	16.21	31.64	4.20	15.18	67.21	70.29
30	15.12	33.04	1.40	10.47	59.93	63.01
40	14.17	31.92	0.84	8.04	55.17	57.97
50	13.25	30.80	0.56	6.55	50.97	53.77
70	11.57	28.28	0.28	4.82	44.80	47.88
100	9.60	25.43	0.06	3.44	38.36	41.72
150	7.45	21.70	0	2.37	31.36	35.00
200	6.08	18.96	0	1.82	26.85	30.52
300	4.48	15.18	0	1.25	20.92	24.84
400	3.56	12.74	0	0.95	17.22	21.00
500	2.97	10.98	0	0.78	14.73	18.31

this is not what we observe in Fig. 3. This divergence at the higher energies, however, is likely to be simply due to the different polarization and absorption potentials used in the atomic optical models for the two leptons (see Sec. III).

Although the energy dependence of our measured and computed positron TCSs is similar, their magnitude is significantly different. The forward-angle-scattering correction does account for some of that discrepancy, but only in part. Specifically, the IAM SCAR results are a factor of 3.4–4.4 larger in magnitude than the corrected experimental data at the common impact energies. This is somewhat surprising, given the quite fair accord we have found between the IAM SCAR calculations and cross sections measured at Trento or the Australian Positron Beamline Facility [26,59,73] for some other large polyatomic molecules. We note, however, that for yet further targets the level of accord was not so good or not uniformly good at all energies [55,58,72]. Nevertheless, this large difference in indole between theory and experiment has only been seen for uracil [27] and in that case the discrepancy was almost certainly caused by inaccuracies in the temperature-vapor pressure curve that were used to derive the pressure from the measurements of the cell temperature. As argued by Chiari *et al.* [58], the success of the IAM SCAR approach seems to be quite species specific. This might be due to the ability of the SCAR formalism to provide an accurate quantum mechanical representation of the target structure in some cases but not in others. We also note that below ∼6 eV the IAM SCAR ICS for the rotational excitations becomes much larger in magnitude than the elastic ICS. Although indole is a very polar molecule and therefore a large rotational excitation cross section is anticipated, its magnitude might be somewhat overestimated at those energies. This follows as those additional dipole-induced excitation cross sections are calculated under the first Born approximation, which is thought to not be fully valid at lower incident energies.

On the experimental side of things, the beam instability we encountered during the indole measurements might be blamed for the larger statistical uncertainties in the data, but cannot be the cause of the large discrepancy we found between theory and experiment in the TCS absolute values (see Fig. 3). In principle, an incorrect reading of the target or background pressure, a wrong calibration of the zero pressure of the baratron, or an anomalously small beam attenuation might all lead to an underestimated TCS. However, the pressure gauge we used in the present experiment is exactly the same as that of our previous studies, the calibration of the baratron zero was accurately checked, and the beam transmittance was always kept at around 0.7. Therefore, none of these effects can explain the discrepancy. We acknowledge that the model for the thermal transpiration correction that we used here might not be fully adequate for this target, given its large molecular size. Unfortunately, we cannot quantitatively estimate what effect this might have on the pressure measurements, although we anticipate that its extent would not be larger than a few percent, i.e., by far smaller than the observed discrepancy. This is confirmed by the comparison of the present measured TCS with a corresponding TCS in pyrimidine (see below), which can be considered a parent molecule of indole.

In order to shed more light on the large discrepancy between theory and experiment in indole and to put the indole results into perspective with respect to the relevant nucleobases, in Fig. 4 we compare the present measured and computed TCSs to a selection of data and calculations for other structurally similar targets. Specifically shown in Fig. 4 are the

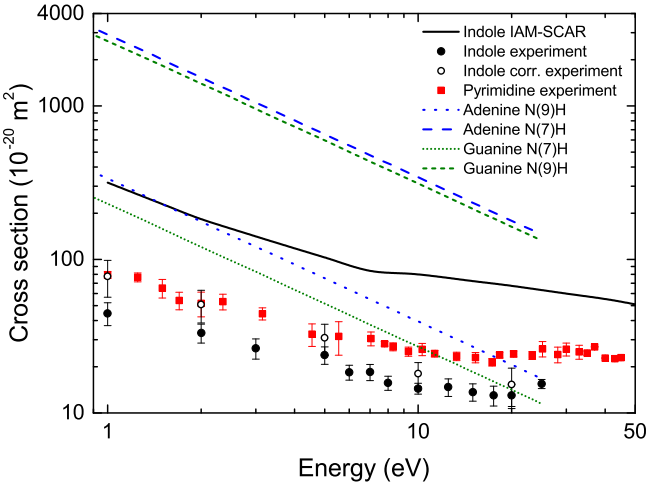

FIG. 4. (Color online) Comparison of the present measured and computed TCSs for positron impact with indole to the TCS for positron-pyrimidine scattering measured by Zecca *et al.* [20] and the elastic ICSs averaged over the rotational excitations for the purine bases adenine and guanine, as calculated by Franz and Gianturco [29]. Shown are the results for the N(7)H and N(9)H tautomers of those nucleobases (see the text).

experimental TCSs of the Trento group for pyrimidine [20] and the elastic ICSs, averaged over the rotational excitations and including the Born-dipole correction, for the purine nucleobases adenine and guanine. Those latter results were calculated using the model potential approach of Franz and Gianturco [29]. In particular, we plot in Fig. 4 the results of Franz and Gianturco [29] for just two each of the adenine and guanine tautomers, namely, those with the hydrogen attached to the nitrogen in either position 7 or 9 of the imidazole ring. The reason for this choice is that N(9)H adenine seems to be the dominant tautomer in the gas phase [74], although there may be trace amounts of the N(7)H tautomer [75]. In respect to guanine, the two lowest-energy tautomers N(7)H and N(9)H have both been found in the gas phase [76].

It is very interesting to see in Fig. 4 that the uncorrected TCS for pyrimidine is somewhat larger in magnitude than the present experimental data for indole at all common energies. This observation is in quite good agreement with the recent finding of Franz and Gianturco [29] that the cross sections for the nucleobases roughly scale with the square of the permanent dipole moments of the target (see Table I). However, we also note that the dipole polarizability of pyrimidine is almost half that of indole (see again Table I). As we observed in some of our previous studies, for the important role played by the target polarizability in the low-energy scattering dynamics for polar molecules (see, for instance, [55,58,71]), we expected that it might be even more important in indole given its very large polarizability. Nonetheless, it does not seem to be the case here. We can speculate that the difference in the pyrimidine and indole TCSs might also be due, at least in part, to their dissimilar structures, namely, a single ring versus a double ring, respectively.

When we compare the indole TCSs with the calculations for the elastic ICSs of the adenine and guanine tautomers, we find a huge difference in magnitude with the adenine N(7)H and guanine N(9)H cross sections. This can easily in the first instance be interpreted in terms of the larger dipole moment of those tautomers, compared to all the other possible tautomers, which is reflected in the much larger magnitude of their cross sections [29]. In respect to the adenine N(9)H and guanine N(7)H tautomers, the present experimental TCSs for indole are smaller in magnitude except at the highest investigated energies, where the calculations do not include any of the open inelastic channels. Given the similarity in the polarizability of indole, adenine, and guanine (Table I), we suspect that the difference in their cross-section magnitude is due to their different dipole moments and chemical composition.

V. CONCLUSION

We have reported on low-energy TCS measurements for positron scattering from indole, an analog of the purine nucleobases. Also presented were IAM SCAR theoretical results of the TCS and ICSs for elastic and inelastic (Ps formation and electronic excitations plus direct ionization) scattering between 1 and 500 eV, as well as some elastic DCSs at selected incident energies. In addition, the electron-impact TCS for indole is also given. The present computed and measured TCSs were both found to dramatically increase in absolute value as the incident energy was reduced. However, a significant magnitude difference was found between theory and experiment, which cannot be fully explained in terms of the forward-angle-scattering effect affecting the measurements. The present TCS measurements not only help, at least in part, to fill a gap in the literature of experimental cross sections for the nucleobases, but also show that positron interactions with the purine nucleobases are significant and must be accounted for in any realistic study of how biomedical techniques, such as positron emission tomography, work at the nanoscale. In particular, it was apparent that the direct ionization cross section for indole is quite large in magnitude, which means that a significant number of secondary electrons may be liberated. Those secondary electrons, for example, through dissociative electron attachment, might then well lead to damage at the cellular level [22–24]. A complete and accurate database of cross sections for the various building blocks of living matter, such as water, the nucleobases, the sugars, and the amino acids, and for all the different scattering processes is therefore crucial for energy deposition models that aim at improving our understanding of radiation damage at the subcellular level. However, much more work is clearly needed in this respect.

In particular, in order to pursue such a long-term plan, the present experimental and theoretical methods need to be improved. In respect to the experimental techniques, third-generation positron spectrometers, such as that at the Australian National University (ANU) [77], already exist and possess both higher incident positron flux and better energy resolution. They also provide direct measurements for other discrete scattering channels, such as the Ps formation ICS and elastic DCSs. Note that those DCSs can in principle be used for the forward-angle-scattering correction to the measured TCSs. However, given that all scattering-cell-based measurements (including differential) are inevitably affected by angular limitations, theoretical calculations are still presently required for that correction. We note that the angular discrimination can be

further improved by using higher-activity radioactive sources and to carefully design the detection region of the apparatus to negotiate a lower beam intensity with a better angular resolution. Future positron spectrometers are also expected to more easily deal with organic molecules that are solid at room temperature. Technical improvements in this direction include the use of a scattering cell that can be heated up to several hundred degrees Celsius, cold traps, and the prospect of heating the entire apparatus at high temperature. The measurements on uracil by Anderson *et al.* at ANU [27] already successfully made use of such a system. In addition, we note that the existence of experimental data, such as those we report here, encourages the development of many different theoretical models, not just the approach we employed in this paper.

On the theoretical side, the range of validity of the current formalism needs to be extended to much lower incident energies. In order to achieve this goal, we are currently developing a multicenter scattering method for low and intermediate energies. A further improvement in our phenomenological approach to Ps formation may also be warranted. However, we note that this is particularly challenging owing to the complex nature of this scattering channel, which cannot be represented in terms of binary collisions. Nevertheless, a semiempirical formula, based on the Ps formation cross sections measured at ANU, could be used in order to more accurately introduce the threshold energy for this scattering process.

The further development of the current theoretical and experimental techniques, as described above, together with an extensive comparative work of complex biomolecules will certainly facilitate the compilation of a complete and accurate cross-section database. This will contribute to our understanding of energy deposition in living matter and eventually lead to an appreciation of the way radiation may induce damage in biological systems.

ACKNOWLEDGMENTS

The experimental work was undertaken under a Memorandum of Understanding between the University of Trento and the Flinders University node of the Australian Research Council Centre of Excellence for Antimatter-Matter Studies. G.G. and F.B. would like to acknowledge the Spanish Ministerio de Economía y Productividad (Project No. FIS2012-31230) and the European Science Foundation (COST Action Grants No. MP1002−Nano-IBCT and No. MC1301-CELINA) for financial support.

[1] G. Garcia Gómez-Tejedor and M. C. Fuss, *Radiation Damage in Biomolecular Systems* (Springer, Berlin, 2012).
[2] United Nations Scientific Committee on the Effects of Atomic Radiation, Sources and Effects of Ionizing Radiation, UNSCEAR 2000 Report to the General Assembly, with Scientific Annexes (United Nations, New York, 2000), Vol. I.
[3] IAEA, *Radiological Protection for Medical Exposure to Ionizing Radiation*, Safety Standards Series No. RS-G-15 (International Atomic Energy Agency, Vienna, 2002).
[4] B. J. McParland, *Medical Radiation Dosimetry* (Springer, London, 2014).
[5] A. Mozumder and Y. Hatano, *Charged Particle and Photon Interactions with Matter: Chemical, Physicochemical, and Biological Consequences with Applications* (CRC, Boca Raton, 2004).
[6] A. G. Sanz, M. C. Fuss, A. Muñoz, F. Blanco, P. Limão-Vieira, M. J. Brunger, S. J. Buckman, and G. García, Int. J. Radiat. Biol. **88**, 71 (2012).
[7] R. D. White, W. Tattersall, G. Boyle, R. E. Robson, S. Dujko, Z. Lj. Petrovic, A. Bankovic, M. J. Brunger, J. P. Sullivan, S. J. Buckman, and G. Garcia, Appl. Radiat. Isotopes **83**, 77 (2014).
[8] J. B. Maljković, A. R. Milosavljević, F. Blanco, D. Šević, G. García, and B. P. Marinković, Phys. Rev. A **79**, 052706 (2009).
[9] P. Palihawadana, J. Sullivan, M. Brunger, C. Winstead, V. McKoy, G. Garcia, F. Blanco, and S. Buckman, Phys. Rev. A **84**, 062702 (2011).
[10] S. M. Bellm, C. J. Colyer, B. Lohmann, and C. Champion, Phys. Rev. A **85**, 022710 (2012).
[11] D. B. Jones, S. M. Bellm, P. Limão-Vieira, and M. J. Brunger, Chem. Phys. Lett. **535**, 30 (2012).
[12] D. B. Jones, S. M. Bellm, F. Blanco, M. Fuss, G. García, P. Limão-Vieira, and M. J. Brunger, J. Chem. Phys. **137**, 074304 (2012).
[13] M. C. Fuss, A. G. Sanz, F. Blanco, J. C. Oller, P. Limão-Vieira, M. J. Brunger, and G. García, Phys. Rev. A **88**, 042702 (2013).
[14] Z. Mašín, J. D. Gorfinkiel, D. B. Jones, S. M. Bellm, and M. J. Brunger, J. Chem. Phys. **136**, 144310 (2012).
[15] P. Mozejko and L. Sanche, Radiat. Environ. Biophys. **42**, 201 (2003).
[16] Z. Tan, Y. Xia, X. Liu, M. Zhao, Y. Ji, F. Li, and B. Huang, Radiat. Environ. Biophys. **43**, 173 (2004).
[17] S. Tonzani and C. H. Greene, J. Chem. Phys. **124**, 054312 (2006).
[18] F. Blanco and G. García, Phys. Lett. A **360**, 707 (2007).
[19] C. Winstead and V. McKoy, Radiat. Phys. Chem. **77**, 1258 (2008).
[20] A. Zecca, L. Chiari, G. García, F. Blanco, E. Trainotti, and M. J. Brunger, J. Phys. B **43**, 215204 (2010).
[21] A. Dora, L. Bryjko, T. van Mourik, and J. Tennyson, J. Chem. Phys. **136**, 024324 (2012).
[22] M. A. Huels, B. Boudaiffa, P. Cloutier, D. Hunting, and L. Sanche, J. Am. Chem. Soc. **125**, 4467 (2003).
[23] A. Dumont, Y. Zheng, D. Hunting, and L. Sanche, J. Chem. Phys. **132**, 045102 (2010).
[24] M. Rezaee, P. Cloutier, A. D. Bass, M. Michaud, D. J. Hunting, and L. Sanche, Phys. Rev. E **86**, 031913 (2012).
[25] E. Surdutovich, G. Setzler, W. E. Kauppila, S. J. Rehse, and T. S. Stein, Phys. Rev. A **77**, 054701 (2008).
[26] P. Palihawadana, R. Boadle, L. Chiari, E. K. Anderson, J. R. Machacek, M. J. Brunger, S. J. Buckman, and J. P. Sullivan, Phys. Rev. A **88**, 012717 (2013).
[27] E. K. Anderson, R. A. Boadle, J. R. Machacek, L. Chiari, C. Makochekanwa, S. J. Buckman, M. J. Brunger, G. Garcia, F. Blanco, O. Ingolfsson, and J. P. Sullivan, J. Chem. Phys. **141**, 034306 (2014).

[28] J. Franz, F. A. Gianturco, and I. Baccarelli, Eur. J. Phys. D **68**, 183 (2014).

[29] J. Franz and F. A. Gianturco, Eur. Phys. J. D **68**, 279 (2014).

[30] A. G. Sanz, M. C. Fuss, F. Blanco, Z. Mašín, J. D. Gorfinkiel, R. P. McEachran, M. J. Brunger, and G. García, Phys. Rev. A **88**, 062704 (2013).

[31] X. Shen, J. Lind, and G. Merenyi, J. Phys. Chem. **91**, 4403 (1987).

[32] S. T. Park, A. Gahlmann, Y. He, J. S. Feenstra, and A. H. Zewail, Angew. Chem. **120**, 9638 (2008).

[33] J. R. Lakowicz, *Principles of Fluorescence Spectroscopy*, 2nd ed. (Plenum, New York, 1999).

[34] N. A. Borisevich, A. L. Ivanov, S. M. Kazakov, A. V. Kukhto (Kukhta), A. I. Mit'kovets, D. V. Murtazaliev, V. A. Povedailo, and O. V. Khristoforov, J. Appl. Spectrosc. **72**, 503 (2005).

[35] A. Modelli, D. Jones, and S. A. Pshenichnyuk, J. Chem. Phys. **139**, 184305 (2013).

[36] A. Zecca, L. Chiari, A. Sarkar, and M. J. Brunger, New J. Phys. **13**, 115001 (2011).

[37] A. Zecca, L. Chiari, A. Sarkar, S. Chattopadhyay, and M. J. Brunger, Nucl. Instrum. Methods Phys. Res. Sect. B **268**, 533 (2010).

[38] J. Šetina, Metrologia **36**, 623 (1999).

[39] A. Zecca, L. Chiari, E. Trainotti, D. V. Fursa, I. Bray, and M. J. Brunger, Eur. Phys. J. D **64**, 317 (2011).

[40] A. Zecca, L. Chiari, E. Trainotti, D. V. Fursa, I. Bray, A. Sarkar, S. Chattopadhyay, K. Ratnavelu, and M. J. Brunger, J. Phys. B **45**, 015203 (2012).

[41] A. Zecca, L. Chiari, E. Trainotti, and M. J. Brunger, J. Phys. B **45**, 085203 (2012).

[42] L. Chiari and A. Zecca, Eur. Phys. J. D **68**, 297 (2014).

[43] A. Zecca and M. J. Brunger, in *Nanoscale Interactions and Their Applications: Essays in Honor of Ian McCarthy*, edited by F. Wang and M. J. Brunger (Research Signpost, Trivandrum, 2007).

[44] A. G. Sanz, M. C. Fuss, F. Blanco, J. D. Gorfinkiel, D. Almeida, F. Ferreira da Silva, P. Limão-Vieira, M. J. Brunger, and G. García, J. Chem. Phys. **139**, 184310 (2013).

[45] O. S. Andersen, D. V. Greathouse, L. L. Providence, M. D. Becker, and R. E. Koeppe, J. Am. Chem. Soc. **120**, 5142 (1998).

[46] G. Yu, X.-R. Huang, W. Chen, and C.-C. Sun, J. Comput. Chem. **32**, 2005 (2011).

[47] J. W. Hager and S. C. Wallace, Anal. Chem. **60**, 5 (1988).

[48] S. Riahi, S. Eynollahi, M. R. Ganjali, and P. Norouzi, Int. J. Electrochem. Sci. **5**, 355 (2010).

[49] V. M. Orlov, A. N. Smirnov, and Y. M. Varshavsky, Tetrahedron Lett. **17**, 4377 (1976).

[50] G. L. Blackman, R. D. Brown, and F. R. Burden, J. Mol. Spectrosc. **35**, 444 (1970).

[51] B. Jansik, D. Jonsson, P. Salek, and H. Agren, J. Chem. Phys. **121**, 7595 (2004).

[52] E. D. Bergmann, Ann. N.Y. Acad. Sci. **158**, 140 (1969).

[53] D. R. Lide, *CRC Handbook of Chemistry and Physics* (CRC, Boca Raton, 2005).

[54] F. Blanco and G. García, J. Phys. B **42**, 145203 (2009).

[55] L. Chiari, E. Anderson, W. Tattersall, J. R. Machacek, P. Palihawadana, C. Makochekanwa, J. P. Sullivan, G. García, F. Blanco, R. P. McEachran, M. J. Brunger, and S. J. Buckman, J. Chem. Phys. **138**, 074301 (2013).

[56] L. Chiari, H. V. Duque, D. B. Jones, P. A. Thorn, Z. Pettifer, G. B. da Silva, P. Limão-Vieira, D. Duflot, M.-J. Hubin-Franskin, J. Delwiche, F. Blanco, G. García, M. C. A. Lopes, K. Ratnavelu, R. D. White, and M. J. Brunger, J. Chem. Phys. **141**, 024301 (2014).

[57] M. C. Fuss, A. G. Sanz, F. Blanco, P. Limão-Vieira, M. J. Brunger, and G. García, Eur. Phys. J. D **68**, 161 (2014).

[58] L. Chiari, A. Zecca, G. García, F. Blanco, and M. J. Brunger, J. Phys. B **47**, 175202 (2014).

[59] L. Chiari, A. Zecca, F. Blanco, G. García, M. V. Perkins, S. J. Buckman, and M. J. Brunger, J. Phys. Chem. A **118**, 6466 (2014).

[60] D. D. Reid and J. M. Wadehra, Phys. Rev. A **50**, 4859 (1994).

[61] D. D. Reid and J. M. Wadehra, J. Phys. B **29**, L127 (1996).

[62] D. D. Reid and J. M. Wadehra, J. Phys. B **30**, 2318 (1997).

[63] R. P. McEachran, D. L. Morgan, A. G. Ryman, and A. D. Stauffer, J. Phys. B **10**, 663 (1977).

[64] L. Chiari, A. Zecca, S. Girardi, E. Trainotti, G. García, F. Blanco, R. P. McEachran, and M. J. Brunger, J. Phys. B **45**, 215206 (2012).

[65] M. E. Riley and D. G. Truhlar, J. Chem. Phys. **63**, 2182 (1975).

[66] X. Z. Zhang, J. F. Sun, and Y. F. Liu, J. Phys. B **25**, 1893 (1992).

[67] G. Staszewska, D. W. Schwenke, D. Thirumalai, and D. G. Truhlar, Phys. Rev. A **28**, 2740 (1983).

[68] L. Chiari, A. Zecca, G. García, F. Blanco, and M. J. Brunger, J. Phys. B **46**, 235202 (2013).

[69] L. Chiari, A. Zecca, E. Trainotti, G. García, F. Blanco, M. H. F. Bettega, S. d. A. Sanchez, M. T. d. N. Varella, M. A. P. Lima, and M. J. Brunger, Phys. Rev. A **88**, 022708 (2013).

[70] M. T. d. N. Varella, S. d. A. Sanchez, M. H. F. Bettega, M. A. P. Lima, L. Chiari, A. Zecca, E. Trainotti, and M. J. Brunger, J. Phys. B **46**, 175202 (2013).

[71] M. J. Brunger and A. Zecca, in *Frontiers in Physics: 3rd International Meeting*, edited by S.-W. Chia, M. R. Muhamad, and K. Ratnavelu, AIP Conf. Proc. No. 1150 (AIP, New York, 2009), p. 68.

[72] L. Chiari, P. Palihawadana, J. R. Machacek, C. Makochekanwa, G. García, F. Blanco, R. P. McEachran, M. J. Brunger, S. J. Buckman, and J. P. Sullivan, J. Chem. Phys. **138**, 074302 (2013).

[73] W. Tattersall, L. Chiari, J. R. Machacek, E. Anderson, R. D. White, M. J. Brunger, S. J. Buckman, G. García, F. Blanco, and J. P. Sullivan, J. Chem. Phys. **140**, 044320 (2014).

[74] C. Plützer and K. Kleinermanns, Phys. Chem. Chem. Phys. **4**, 4877 (2002).

[75] M. J. Nowak, H. Rostkowska, L. Lapinski, J. S. Kwiatkowski, and J. Leszczynski, J. Phys. Chem. **98**, 2813 (1994).

[76] W. Chin, M. Mons, I. Dimicoli, F. Piuzzi, B. Tardivel, and M. Elhanine, Eur. Phys. J. D **20**, 347 (2002).

[77] J. P. Sullivan, A. Jones, P. Caradonna, C. Makochekanwa, and S. J. Buckman, Rev. Sci. Instrum. **79**, 113105 (2008).